machines

Article

DP-Climb: A Hybrid Adhesion Climbing Robot Design and Analysis for Internal Transition

Qingfang Zhang, Xueshan Gao *, Mingkang Li, Yi Wei and Peng Liang

School of Mechatronical Engineering, Beijing Institute of Technology, Beijing 100081, China
* Correspondence: xueshan.gao@bit.edu.cn

Abstract: This paper proposes a double propeller wall-climbing robot (DP-Climb) with a hybrid adhesion system based on the biomimetic design principle to address the problems of single adhesion-powered wall climbing robots (WCRs). Such problems include poor maneuverability and adaptability to orthogonal working surfaces with different roughness and flatness, weak flexibility of ground-wall transition motion, and easy stand stilling of transition. Based on the clinging characteristics of different creatures, the hybrid system combines the rotor units' reverse thrust, the drive wheels' driving torque, and the adhesion force offered by the coating material to power the robot through a coupled control strategy. Based on the Newton–Euler equations, the robot's kinematic characteristics during the ground-wall internal transition motion were analyzed, the safe adhesion conditions were obtained, and a dynamics model of the robot's ground-wall transition was established. This provided the basis for the coupling control between different power units. Finally, an internal transition PID control strategy based on DP-Climb was proposed. Through mechanical and aerodynamic characteristic experiments, it is verified that the robot's actual output pulling force can meet the transition motion demand. The experimental results show that the proposed strategy can enable the DP-Climb to complete the ground-wall mutual transition motion smoothly with a speed of 0.12 m/s. The robot's maximum wall motion speed can reach 0.45 m/s, which verifies that the hybrid adhesion system can flexibly and quickly reach the specified position in a target area flexibly and quickly. The robustness and adaptability of WCR to complex application environments are improved.

Keywords: hybrid adhesion system; wall-climbing robot; transition control strategy

Citation: Zhang, Q.; Gao, X.; Li, M.; Wei, Y.; Liang, P. DP-Climb: A Hybrid Adhesion Climbing Robot Design and Analysis for Internal Transition. *Machines* **2022**, *10*, 678. https://doi.org/10.3390/machines10080678

Academic Editor: Dan Zhang

Received: 8 July 2022
Accepted: 9 August 2022
Published: 10 August 2022

1. Introduction

As an important branch of special robots, wall-climbing robots (WCRs) can replace humans in high-risk or hard-to-reach environments to perform tasks such as environmental detection and location reconnaissance and assist in disaster rescue, which can ensure the safety of operators and reduce risks and costs. It has important application value in military and civilian fields [1,2]. For emergencies such as fires and earthquakes that occur in a dense urban high-rise building environment, it is particularly necessary to develop a WCR with strong environmental adaptability, the ability to move flexibly on walls of different roughness and damage, and to move freely within a designated target working area and to quickly reach the designated location to obtain the on-site information [3].

WCR has two basic abilities: adhesion and climbing. The stable adhesion of the robot to the wall mainly relies on its adhesion system. The adhesion method of WCR can be mainly divided into magnetic adhesion [4], vacuum suction cups [5], bionic materials and bionic hook and claw spine adhesion [6,7] and reverse thrust adhesion [8]. Magnetic WCR [9] has a strong adhesion force on the wall surface, but it can only be applied to metal contact surfaces, such as oil tanks. The vacuum suction cup-type WCR [10] can form a closed chamber to generate a vacuum with a strong adhesion force and can adapt to different material walls, but it can only be applied to a flat wall surface. The dry-adhesive bionic wall-climbing robot [11,12] can adapt to uneven vertical surfaces but requires frequent cleaning and maintenance, and its moving speed is limited. The hook-claw-type bionic WCR [13] can be used repeatedly, but it can damage the wall, and its adaptability to smooth walls such as glass is weak. Negative pressure-type WCR [14] can adapt to contact walls with different roughness and flatness, has good obstacle-crossing performance, can be reused, does not damage the building surface, and is more suitable for urban high-rise buildings and narrow alleyways and other environments. We compared the wall motion speed and weight properties of negative pressure adhesion WCRs [15–26] developed recently, as shown in Figure 1.

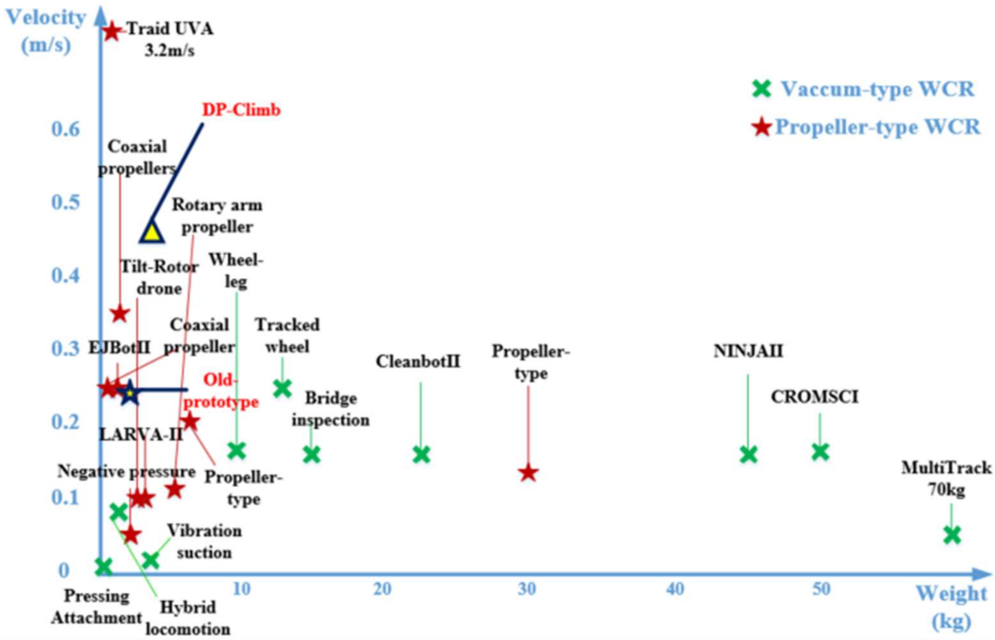

Figure 1. Property comparison of negative pressure WCRs.

According to Figure 1, propeller-type WCRs move faster on the wall and have a relatively smaller mass. Therefore, this paper designs a double propeller wall climbing robot based on the functional principle of bionic mechanical design to solve the problems of the current WCR. These include attitude adjustment that takes a long time during the transition of the ground-wall internal surface, the weak adaptability to the contact surface with different roughness and flatness, and the easy overturning of the body, which imitates the indirect flight mechanism of lepidopteran insects. When the rotor starts to rotate, the air will form a pressure difference at the upper and lower interfaces of the propeller to make the robot press against the wall. By changing the pitch angle of the rotor, the robot's motion direction can be changed to achieve wall forward and backward or static attachment action [27]. However, in the old version of WCR, which mainly uses the reverse thrust of the propeller and front drive wheels as the power, the robot appears to have a tail-flicking situation during the movement process, and it adopts an open-loop system to control the robot [28]. In practical applications, achieving accurate control of the robot on the wall surface is difficult. When the WCR needs to perform transition motion from the ground surface to the vertical wall surface, the robot is prone to appear the phenomenon of robot overturning due to stuck or excessive inclination. The lack of rolling joints of the rotor makes it difficult to meet the upward force necessary for the robot to turn and walk on the wall, making it easy to slip off. To solve this problem, Alkalla Mohamed G developed Erbo [29,30]. The two coaxial propellers provide sufficient adhesion force, but the robot motion is limited when the ground-wall transition is carried out by lifting the robot with an external joint. Myeong [31] used a multi-axis rotorcraft to hover on the wall after taking off from the ground. However, due to unpredictable wind gusts, the WCRs such as UVA will be difficult to land, and the internal drone attitude will be significantly affected in the event of a collision. With long lead times for precise positioning, the camera-mounted picture is difficult to capture, and it may even collide with the wall and damage the robot.

The flexible and fast movement of the WCR on the wall is also related to the movement mechanism of the robot. The commonly used movement methods can be classified as wheeled [32,33], crawler [34] and legged [35]. The crawler-type WCR moves faster, but the weight is generally heavier, and the crawler can cause malfunctions when encountering small obstacles. At the same time, legged structures have better obstacle-crossing performance, but the flexibility is weak, and the control is relatively complicated. Therefore, the WCR designed in this paper simplifies the limbs of the gecko into a wheeled mechanism to realize the functions of rapid movement and positioning of the robot.

This paper will design a double propeller wall climbing robot(DP-Climb) with a hybrid adhesion system that can be internally transitioned based on the principle of biomimetic design from the perspective of robot dynamics. It aims to enhance the mobility and adaptability of WCR to complex application environments, make up for the shortcomings of a single adhesion-powered WCR [36], reduce the time consumed for an attitude adjustment, and increase the endurance of the robot. The hybrid adhesion system of DP-Climb combines the clinging characteristics of different creatures. It is mainly composed of two symmetrical rotor units that imitate flapping wings and two rear drive wheels that imitate animal hind limbs. At the same time, a coating material that can enhance the friction coefficient between the wheel body and the wall surface is used on the wheel body to imitate the adhesion characteristics of the gecko feet. The three coupling controls jointly provide the adhesion and traction force required by the robot movement so that the robot can have a certain obstacle crossing ability, and the robot can move flexibly and quickly on contact surfaces of different materials and flatness without being disturbed by factors such as wall cracks, surface protrusions or holes. In addition, the DP-Climb hybrid adhesion system can help the robot adjust the ground-wall transition attitude quickly, reduce energy consumption, improve the endurance of the robot, shorten the positioning time, and enhance its stability. The main contributions of this study are as follows:

(1) A WCR with a hybrid adhesion system is designed based on the principle of biomimetic design. To solve the above problems, this manuscript designs DP-Climb, a double propeller wall climbing robot with a hybrid adhesion system. The robot uses symmetrical rotor bionic joints to adjust the pitch and roll angle of the rotor joints in real-time according to the robot's attitude. It also adopts the skeleton design to optimize the rotor fixed disk to reduce the airflow loss, utilizes the hind limb drive bionic joints to reduce the tailing of the robot and applies the coating material to improve the adhesion force of the robot. It obtains the ground-wall dynamic model of the robot based on the Newton–Euler equation. The dynamic model provides a theoretical basis for the transition motion control of the robot.

(2) A PID motion control strategy for the ground-wall internal transition based on DP-Climb is proposed. The paper designs the ground-wall PID control strategy of the robot based on the dynamic model obtained. It also realizes the autonomy of the robot through PID closed-loop control, which effectively improves the robot's autonomous motion capability and control accuracy and stability. To obtain the dynamic characteristics of the key power unit of the robot, an experimental platform for the mechanical characteristics and aerodynamic characteristics is designed, and the appropriate wheel surface coating material is selected through the tensile force test experiment and the repeatability test experiment of the attachment materials. The functional relationship between the robot's rotor power unit's current output and the actual tensile force output is obtained to compensate for the adhesion dynamic error caused by the airflow loss. The feasibility of the transition control strategy of DP-Climb with a hybrid adhesion system is verified by simulations and experiments.

The structure of this paper is as follows. Section 2 introduces the design scheme of the robot adhesion system. Section 3 establishes the dynamic model of the robot's transition motion process and discusses the control strategy of the robot's ground-wall internal transition in detail. Section 4 presents the simulation and experimental results to verify that DP-Climb can fast transition between the ground and the wall. Finally, the summary conclusions and an outlook for future work are provided in Section 5.

2. Materials and Methods

The DP-Climb adhesion system is designed based on the principle of biomimetic design using a hybrid dynamic adhesion system. The hybrid system consists of the reverse thrust generated by the rotor units, the driving force provided by the drive wheels, and the adhesion force provided by the coating material, which together powers the robot through a coupled control strategy. The hybrid adhesion mechanism of DP-Climb is shown in Figure 2.

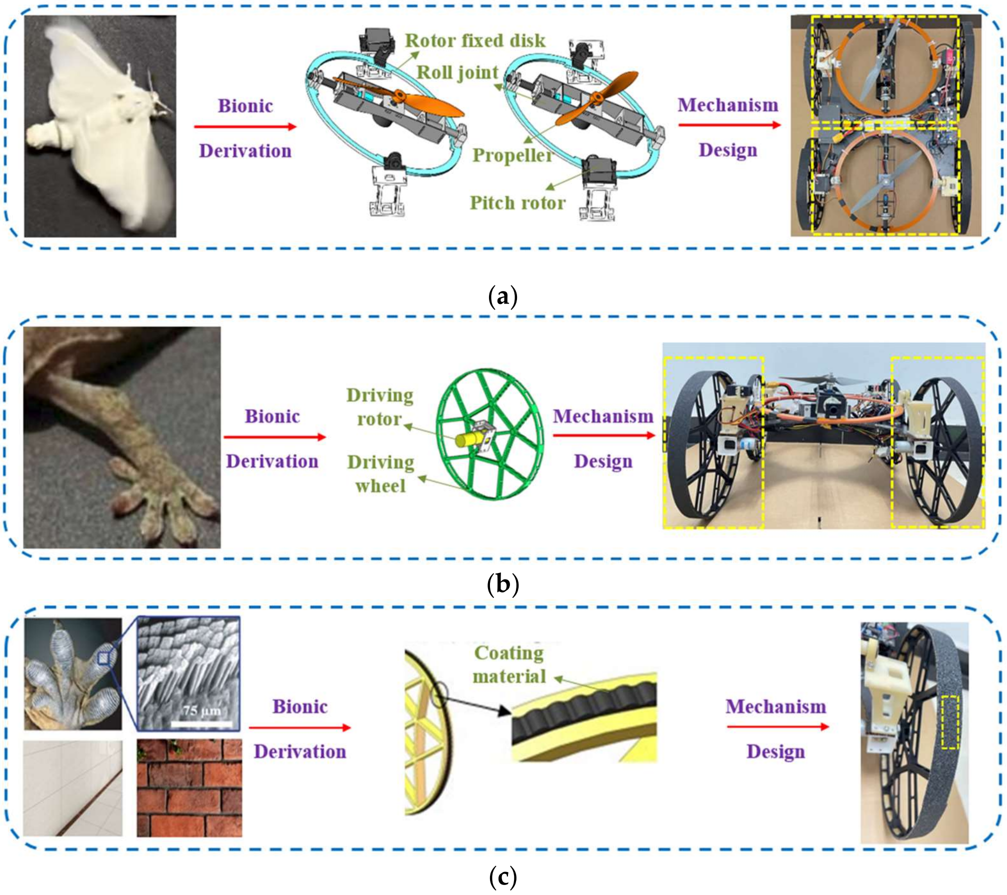

Figure 2. Design of DP-Climb hybrid adhesion system: (**a**) symmetrical rotor bionic joints; (**b**) hind limb drive bionic joints (**c**) a coating material to enhance the friction.

Lepidopteran insects such as moths fly indirectly in the air and change the direction of airflow by changing their own pitch angle. Therefore, to further improve the effective adhesion force of the rotor system, after selecting the 10-inch propellers and 1250 KV type brushless motors, two symmetrical rotor joints were designed to be mounted on the rotor fixed disk with reference to the flutter wing configuration. The rotor joints can change the reverse thrust of the robot through roll joints and pitch rotors according to the different wall postures of the robot to provide the corresponding adhesion force and traction force, as shown in Figure 2a.

When animals such as geckos transition from the ground to the wall, their limbs, especially the hind limbs, need to provide sufficient upward force. Through the technical means of bionic derivation, the limbs of the gecko can be simplified into a wheel body that can move flexibly, and the rear-wheel drive is used to provide the driving torque for the robot to climb upward. The structure is shown in Figure 2b.

In addition, the gecko has an extraordinary climbing ability through many multi-scale hierarchical structures. The Van der Waals force and other types of noncovalent forces (such as capillary forces) enable it to adhere to different types of contact surfaces, and many dry adhesive materials have been developed for climbing [37,38]. A special coating material was added to the wheel's surface to enhance the friction coefficient between the robot and the wall surface and generate a larger friction force to assist the robot in moving on the wall surface, as indicated in Figure 2c.

3. Results

3.1. Analysis of Safe Adhesive Conditions for DP-Climb Transition

WCR works mainly on different building surfaces in cities. Therefore, the robot needs to achieve stable adhesion on walls with different materials and flatness while having sufficient mobility to walk between the ground and the vertical wall surfaces.

To achieve this purpose, it is first necessary to analyze the safe adhesion conditions of the WCR ground-wall transition process. A three-dimensional global coordinate system $\{XYZO\}$ and a three-dimensional robot coordinate system $\{xyzc\}$ are established. c is the centroid of the robot, α_{10} and α_{20} represent the angle between the rotor fixed disk and the ground, respectively, α_1 and α_2 represent the angle between the reverse thrust of the rotor and the robot body, respectively, β is the pitch angle of the robot body, αs_1 and αs_2 indicate the pitch angle of the front and rear rotor fixed disks relative to the robot body, respectively, and v is the movement direction of the robot. The kinematic characteristics of DP-Climb in the ground-wall transition are shown in Figure 3.

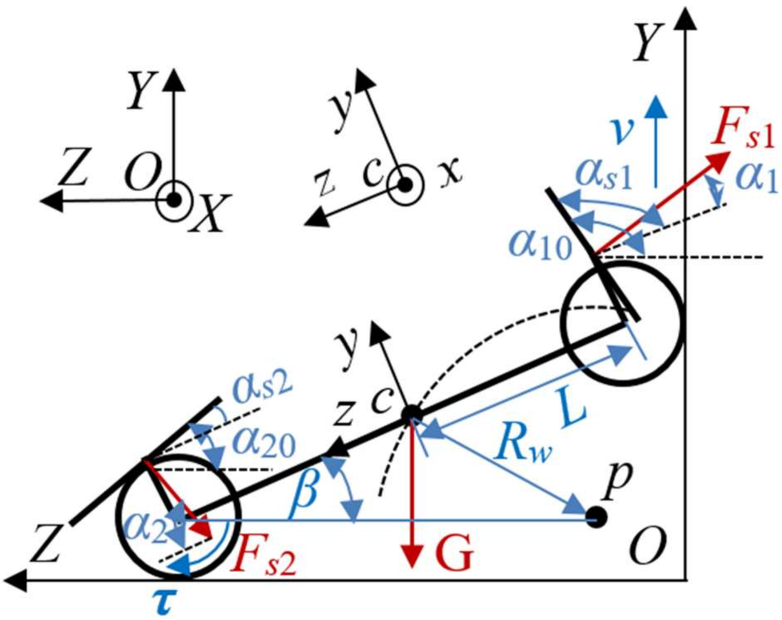

Figure 3. Kinematics model of DP-Climb internal transition.

Assume that the longitudinal and lateral slips of the robot are not considered under pure rolling conditions. It is assumed that (1) the body of DP-Climb is rigid and wheel deformation is neglected; (2) the contact wall of the robot is solid and wall deformation is neglected, and the four wheels are always in vertical contact with the contact surface, and there is only one contact point between each wheel and the surface; (3) the gravity distribution of the contact points between wheels and the surface is uniform; and (4) the robot is in a stable motion state.

The problem of adhesion conditions for the transition motion of DP-Climb can be transformed into the sliding problem of the ladder. In the process of robot ground-wall transition, DP-Climb is symmetrically arranged, c is the center of the robot's mass, p is the center of the robot's transition motion circle, and R_w is the radius of the robot's transition motion. It can be concluded that the slope of the motion trajectory at c is the time-varying situation of the robot's pitch angle β during the ground-wall transition process. The motion trajectory of point c is:

$$(y_c - R_w)^2 + (z_c - R_w)^2 = L^2, \tag{1}$$

where, (z_c, y_c) is the coordinate of the centroid c in the coordinate plane YZO, and the pitch angle β of DP-Climb during the whole ground-wall transition can be obtained as follows:

$$tan\beta = \frac{R_w - z_c}{y_c - R_w}, \tag{2}$$

where, in the process of robot ground-wall transition, i.e., $\beta \in (0, 90)^\circ$, $0^\circ \leq |\alpha_1, \alpha_2| \leq 90^\circ$, the robot pitch angle $\tan\beta$ is a continuous derivable function with respect to time t. When the positive pressure of the reverse thrust on the wall surface completely provides adhesion force for the robot, α_1, α_2 = 0°, when the reverse thrust completely provides upward lift force for the robot, α_1, α_2 = 90°. By analyzing the motion characteristics of DP-Climb, the safe adhesion conditions for the robot to cross the dead point in the ground-wall transition motion without front wheel overturning can be obtained:

$$\begin{cases} \theta_1 = \alpha_1 + \beta = \alpha_{10} - 90 = \alpha_{S1} - 90 + \beta \\ \theta_2 = \alpha_2 - \beta = 90 - \alpha_{20} = 90 - \alpha_{S2} - \beta \\ F_{S1}\cos\theta_1 > F_{S1}\sin\theta_1 > 0, (\theta_1 > 0) \\ F_{S1}\cos\theta_1 \geq F_{S1}\sin\theta_1 > 0, (\theta_1 = 0) \\ |F_{S2}\cos\theta_1| \geq |F_{S2}\sin\theta_1| > 0 \end{cases}. \tag{3}$$

In the robot ground-wall transition process, the front rotor platform plays a critical role. The front rotor platform of the robot needs to provide sufficient upward traction while ensuring a necessary adhesion force. Therefore, to ensure DP-Climb safety, the pitch angle of the robot needs to comply with $100^\circ \leq \alpha_{10} \leq 130^\circ$ during the transition process. If α_{10} is too small, the robot will not receive enough upward component force, and the robot will be stuck and cannot continue the ground-wall transition. If α_{10} is too large, the robot will overturn during the transition movement according to the torque at the origin point O around the X-axis.

3.2. Dynamic Modeling of DP-Climb Internal Transition

Due to the particularity of DP-Climb working on perpendicular intersecting planes, the adhesion force of the robot is easily affected by the wall environment, and the wall motion resistance also changes accordingly, which changes the wall adhesion conditions and kinematic characteristics of the robot. To obtain a more accurate dynamic model of the robot's internal transition motion, it is necessary to analyze the adhesion force, the driving torque, and the friction state between the driving wheel and the wall surface of the robot to provide a theoretical basis for the robot's motion control.

The support force of each wheel on the wall surface is not only affected by the robot's reverse thrust, but the robot's gravity and inertial force will also generate a moment on the center of mass c when the robot moves on the wall surface. Therefore, the effects of gravity, inertial force and reverse thrust should be considered separately. Then, the three solved supporting force components are superimposed to obtain the resultant force of the supporting force of each wheel to solve the dynamic equation of the motion of the centroid c of the robot on the surface. Figure 4 shows the force state analysis of DP-Climb during the ground-wall transition movement.

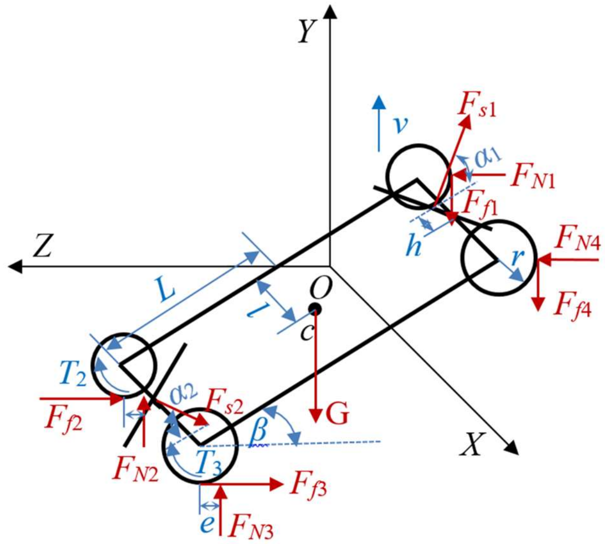

Figure 4. Dynamic analysis of DP-Climb internal transition.

2 L represents the length of the robot's body, which is also the distance between the front and rear wheels, 2 l represents the left and right wheel distances, h represents the vertical distance between the rotor fixed platform and the body, r represents the wheel radius, and e/r represents the wheel rolling resistance coefficient. F_{s1} and F_{s2} represent the reverse thrust provided by the front and rear rotor units of the robot, respectively, F_{Ni} (i = 1, 2, 3, 4) represents the positive pressures of each wheel, F_{fi} represents the sliding friction force on each wheel, G represents the total gravity of the robot, $\boldsymbol{\tau}$ is the driving torque of the driving wheels, which is [T_2 T_3], and T_2 and T_3 are the driving torques of the left and right rear wheels, respectively. Simplifying the wheel model of the robot, the longitudinal adhesion coefficient of each wheel on the wall is μ_i, and M_{fi} represents the rolling resistance moment of each wheel. Since the value of e is very small, it can be neglected in the positive pressure analysis of each wheel. The resultant forces of DP-Climb along each coordinate axis of $\{XYZO\}$ are:

$$\begin{cases} m\ddot{y} = -\mathrm{G} + F_{s1}\sin(\alpha_1+\beta) - F_{s2}\sin(\alpha_2-\beta) + (F_{N2}+F_{N3}) - (\mu_1 F_{N1} + \mu_4 F_{N4}) \\ m\ddot{z} = -F_{s1}\cos(\alpha_1+\beta) - F_{s2}\cos(\alpha_2-\beta) + (F_{N1}+F_{N4}) - (\mu_2 F_{N2} + \mu_3 F_{N3}) \\ (F_{N1}-F_{N4})l + (\mu_3 F_{N3} - \mu_2 F_{N2})l = 0 \\ (F_{N3}-F_{N2})l + (\mu_1 F_{N1} - \mu_4 F_{N4})l = 0 \end{cases}. \quad (4)$$

If the robot does not slip sideways and flip sideways, then $\mu_a = \mu_1 = \mu_4$ and $\mu_b = \mu_2 = \mu_3$. The dynamic equation of DP-Climb in the robot coordinate system $\{xyzc\}$ can be obtained:

$$\begin{cases} ma_{yc} = & F_{sl}\sin\alpha_l - F_{s2}\sin\alpha_2 - \mathrm{G}\cos\beta - 2(\mu_a\cos\beta - \sin\beta)F_{Nl} - 2(\mu_b\sin\beta - \cos\beta)F_{N2} \\ ma_{zc} = & -F_{sl}\cos\alpha_l - F_{s2}\cos\alpha_2 + \mathrm{G}\sin\beta + 2(\mu_a\sin\beta + \cos\beta)F_{Nl} - 2(\mu_b\cos\beta + \sin\beta)F_{N2} \\ m\ddot{y} = & ma_{zc}\sin\beta \\ m\ddot{z} = & ma_{zc}\cos\beta \\ J\ddot{\beta} = & (F_{N1}+F_{N4})L\sin\beta - (F_{N2}+F_{N3})L\cos\beta \\ & +\mu_b(F_{N2}+F_{N3})(L\sin\beta + r) - \mu_a(F_{N1}+F_{N4})(L\cos + r) \\ & -F_{s1}\cos(\alpha_1+\beta)(L\sin\beta + h\cos\beta) + F_{s2}\cos(\alpha_2-\beta)(L\sin\beta - h\cos\beta) \\ & +F_{s1}\sin(\alpha_1+\beta)(L\cos\beta + h\sin\beta) + F_{s2}\cos(\alpha_2-\beta)(L\cos\beta + h\sin\beta) \\ & +\left(M_{f2}+M_{f3}\right) + \left(M_{f1}+M_{f4}\right) \end{cases}, \quad (5)$$

where, I represents the total moment of inertia of the robot. a_{yc} = 0. Combining Equations (4) and (5), the positive pressure of robot wheels can be obtained as:

$$\begin{cases} a_1 = \mu_a \cos\beta + \sin\beta,\ a_2 = \mu_b \sin\beta + \cos\beta \\ a_3 = \sin\theta_1 \cos\beta + \cos\theta_1 \sin\beta,\ a_4 = \sin\theta_2 \cos\beta - \cos\theta_2 \sin\beta \\ b_1 = \mu_a \cos\beta - \sin\beta,\ b_2 = \mu_b \sin\beta - \cos\beta,\ b_3 = \sin 2\beta(\mu_b\mu_a - 1) \\ F_{N4} = F_{N1} = \frac{1}{2}\begin{bmatrix} \left(\frac{a_3}{a_1} + \frac{a_2 \sin\alpha_1}{b_3} - \frac{a_2 a_3 b_1}{a_1 b_3}\right)F_{s1} - \left(\frac{a_4}{a_1} + \frac{a_2 \sin\alpha_2}{b_3} - \frac{a_2 a_4 b_1}{a_1 b_3}\right)F_{s2} \\ -\left(\frac{1}{a_1} + \frac{a_2}{b_3} - \frac{a_2 b_1}{a_1 b_3}\right)\mathrm{G}\cos\beta \end{bmatrix} \\ F_{N3} = F_{N2} = \frac{1}{2}\left[\left(\frac{a_1 \sin\alpha_1}{b_3} - \frac{a_3 b_1}{b_3}\right)F_{s1} - \left(\frac{a_2 \sin\alpha_2}{b_3} - \frac{a_4 b_1}{b_3}\right)F_{s2} - \left(\frac{a_1}{b_3} - \frac{b_1}{b_3}\mathrm{G}\cos\beta\right)\right] \end{cases}. \quad (6)$$

Since the robot performs the ground-wall transition motion at an almost uniform speed, the angular acceleration of each wheel can be approximated to 0. According to the Newton–Euler equations, the dynamic model of DP-Climb can be obtained as:

$$\begin{cases} c_1 &= \sin\theta_1 - \mu_a \frac{a_3}{a_1} - \frac{\mu_a a_2 \sin\alpha_1 - a_1 \sin\alpha_1 + a_3 b_1}{b_3} + \frac{\mu_a a_2 a_3 b_1}{a_1 b_3} \\ c_2 &= \sin\theta_2 - \mu_a \frac{a_4}{a_1} - \frac{\mu_a a_2 \sin\alpha_2 - a_2 \sin\alpha_2 - a_4 b_1}{b_3} + \frac{\mu_a a_2 a_4 b_1}{a_1 b_3} \\ c_3 &= \left[1 - \frac{\mu_a \cos\beta}{a_1} - \frac{\mu_a a_2 - a_1 - b_1}{b_3}\cos\beta + \frac{\mu_a a_2 b_1}{a_1 b_3}\cos\beta\right] \\ c_4 &= -\cos\theta_1 + \frac{a_3}{a_1} + \frac{a_2 \sin\alpha_1}{b_3} - \frac{a_2 a_3 b_1}{a_1 b_3} \\ c_5 &= \cos\theta_2 + \frac{a_4}{a_1} + \frac{a_2 \sin\alpha_2}{b_3} - \frac{a_2 a_4 b_1}{a_1 b_3} \\ c_6 &= \frac{1}{a_1} + \frac{a_2}{b_3} - \frac{a_2 b_1}{a_1 b_4} \\ d_1 &= \sin\theta_1(L\cos\beta - h\sin\beta) - \cos\theta_1(L\sin\beta + h\cos\beta) + \left(\frac{a_3}{a_1} + \frac{a_2 \sin\alpha_1}{b_3} - \frac{a_2 a_3 b_1}{a_1 b_3}\right)L\sin\beta \\ &\quad -\left(\frac{a_1 \sin\alpha_1}{b_3} - \frac{a_3 b_1}{b_3}\right)L\cos\beta - \left(\frac{a_3}{a_1} + \frac{a_2 \sin\alpha_1}{b_3} - \frac{a_2 a_3 b_1}{a_1 b_3}\right)(\mu_a L\cos\beta + \mu_a r) \\ &\quad +\left(\frac{a_3}{a_1} + \frac{a_2 \sin\alpha_1}{b_3} - \frac{a_2 a_3 b_1}{a_1 b_3}\right)\frac{e}{r} + \left(\frac{a_1 \sin\alpha_1}{b_3} - \frac{a_3 b_1}{b_3}\right)\frac{e}{r} \\ d_2 &= \sin\theta_2(L\cos\beta + h\sin\beta) - \cos\theta_2(L\sin\beta - h\cos\beta) - \left(\frac{a_4}{a_1} + \frac{a_2 \sin\alpha_2}{b_3} - \frac{a_2 a_4 b_1}{a_1 b_3}\right)L\sin\beta \\ &\quad +\left(\frac{a_2 \sin\alpha_2}{b_3} - \frac{a_4 b_1}{b_3}\right)L\cos\beta + \left(\frac{a_4}{a_1} + \frac{a_2 \sin\alpha_2}{b_3} - \frac{a_2 a_4 b_1}{a_1 b_3}\right)(\mu_a L\cos\beta + \mu_a r) \\ &\quad -\left(\frac{a_4}{a_1} + \frac{a_2 \sin\alpha_2}{b_3} - \frac{a_2 a_4 b_1}{a_1 b_3}\right)\frac{e}{r} - \left(\frac{a_1 \sin\alpha_2}{b_3} - \frac{a_4 b_1}{b_3}\right)\frac{e}{r} \\ d_3 &= -\left(\frac{1}{a_1} + \frac{a_2}{b_3} - \frac{a_2 b_1}{a_1 b_3}\right)\left[L\sin\beta - \mu_a(L\cos\beta + r) + \frac{e}{r}\right] + \left(\frac{a_1}{b_3} - \frac{b_1}{b_3}\right)\left(L\cos\beta - \frac{e}{r}\right) \\ m\ddot{y} &= c_1 F_{s1} - c_2 F_{s2} - c_3 \mathrm{G} \\ m\ddot{z} &= c_4 F_{s1} - c_5 F_{s2} - c_6 \cos\beta \mathrm{G} - \frac{T_2 + T_3}{r + e} \\ I\ddot{\beta} &= d_1 F_{s1} - d_2 F_{s2} - d_3 \cos\beta \mathrm{G} + \frac{T_2 + T_3}{r + e}(L\sin\beta + r) \end{cases} \quad (7)$$

The expression of the DP-Climb dynamic model can be obtained as follows:

$$\boldsymbol{M}(q)\ddot{\boldsymbol{q}} + \boldsymbol{E}(q)\boldsymbol{F}_s + \boldsymbol{D}\mathrm{G} = \boldsymbol{B}(q)\boldsymbol{\tau}, \quad (8)$$

where, $\boldsymbol{q}$ = $[y\ z\ \beta]^{\mathrm{T}}$, $\boldsymbol{F}s$ = $[F_{s1}\ F_{s2}]^{\mathrm{T}}$. Each coefficient matrix is:

$$\boldsymbol{M}(q) = \begin{bmatrix} m & 0 & 0 \\ 0 & m & 0 \\ 0 & 0 & I \end{bmatrix},\ \boldsymbol{E}(q) = \begin{bmatrix} -c_1 & c_2 \\ -c_4 & c_5 \\ -d_1 & -d_2 \end{bmatrix},\ D = \begin{bmatrix} c_3 \\ c_6\cos\beta \\ d_3\cos\beta \end{bmatrix},\ \boldsymbol{B}(q) = \begin{bmatrix} 0 & 0 \\ -\frac{1}{r+e} & -\frac{1}{r+e} \\ \frac{L\sin\beta + r}{r+e} & \frac{L\sin\beta + r}{r+e} \end{bmatrix}$$

3.3. Control Strategy of DP-Climb Internal Transition

3.3.1. Selection of Wheel Surface Adhesive Material

According to the analysis in the previous section, the adhesion coefficient between the wheel and contact surface is one of the important factors affecting the adhesion of the robot to the wall surface. Therefore, to increase the adhesion between the robot and the contact surface, it is necessary to choose a material with good repeatability and a high friction coefficient as the robot wheel body surface adhesion coating.

Through the collection of various coating materials suitable for the surface of the wheel body and the analysis of the material characteristics, this paper selects several adhesion materials that can meet the task requirements of the robot with better performance for comparison. In a windless indoor environment, an experimental platform for mechanical characteristics was set up to test the upward lift force of the robot and the adhesion force perpendicular to the wall surface using a lime medium wall as the contact surface. The established dynamic model was used to measure the friction coefficients of different adhesive materials on the wheel surface of the robot. To test the repetition rate of the adhesive materials, 10 tensile tests were repeated for each material. The experimental platform for mechanical properties is shown in Figure 5, and the experimental results are shown in Table 1.

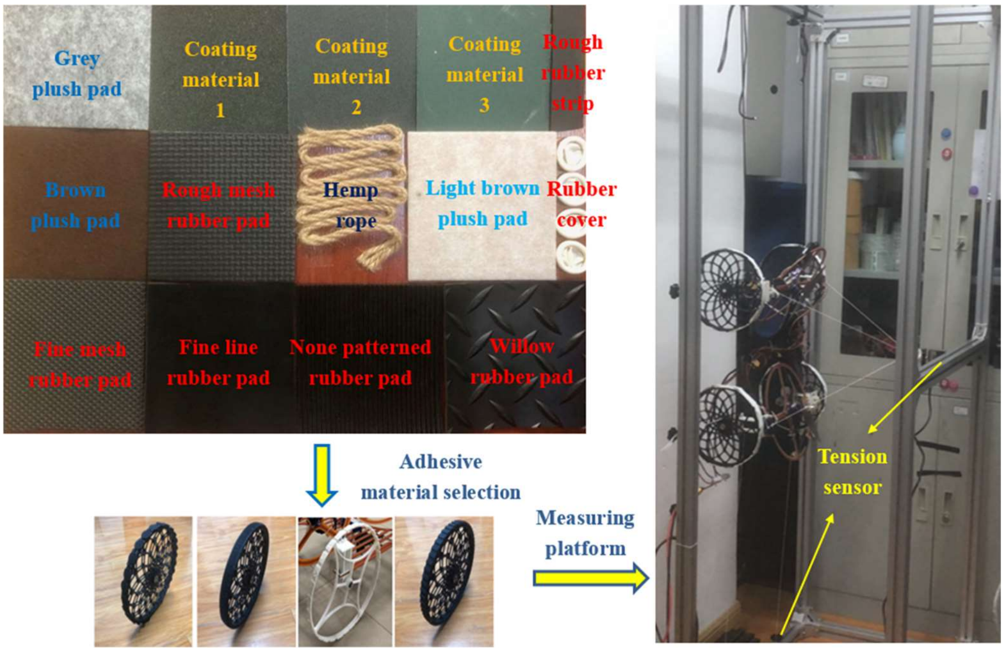

Figure 5. Selection of different adhesive materials for wheel surfaces.

Table 1. Comparison of material properties of different adhesive materials for wheel surface.

Adhesive Material	Coefficient of Friction	Repetition Rate	Adhesive Material	Coefficient of Friction	Repetition Rate
Gray plush pad	0.55	0.90	Hemp rope	0.46	1.00
Coating material 1	0.81	1.00	Light brown plush pad	0.40	0.90
Coating material 2	0.77	0.80	Rubber cover	0.75	0.40
Coating material 3	0.81	0.50	Fine mesh rubber pad	0.40	1.00
Rough rubber strip	0.56	1.00	Fine line rubber pad	0.56	1.00
Brown plush pad	0.54	1.00	Non-patterned rubber pad	0.55	1.00
Rough mesh rubber pad	0.45	1.00	Willow rubber pad	0.59	1.00

Analysis of Table 1 shows that coating material 1 has a relatively large friction coefficient and a high repetition rate, and the comprehensive performance is the best. Therefore, this material will be used as the adhesion material on the surface of the robot wheel body in subsequent research work.

3.3.2. Control Strategy of DP-Climb Ground-Wall Transition

Equation (7) shows that when the robot performs the ground-wall transition at a nearly uniform speed, $m = 3.3$ kg, $r = 0.14$ m, $L = 0.18$ m, $h = 0.08$ m, $l = 0.23$ m, and $\mu_a = 0.81$. During the DP-Climb transition process, the robot can complete the transition motion by changing the pitch joint angle of the front and rear rotor platforms of the robot according to the pitch angle of the fuselage. According to the DP-Climb dynamic model analysis, the relationship between the pitch angle of the rotor platform and the pitch angle of the fuselage is as follows:

$$\begin{cases} \alpha_{s1} = \alpha_{10} - \beta \\ \alpha_{s2} = 180 - \alpha_{10} \end{cases}. \tag{9}$$

The red vectors represent the reverse thrust provided by the front and rear rotor units, F_{s1} and F_{s2}, respectively, and the blue angle indicates the robot pitch angle β. Based on the stable adhesion conditions of the ground-wall transition motion of the robot analyzed above, the robot's ground-wall internal transition motion strategy is designed, as shown in Figure 6.

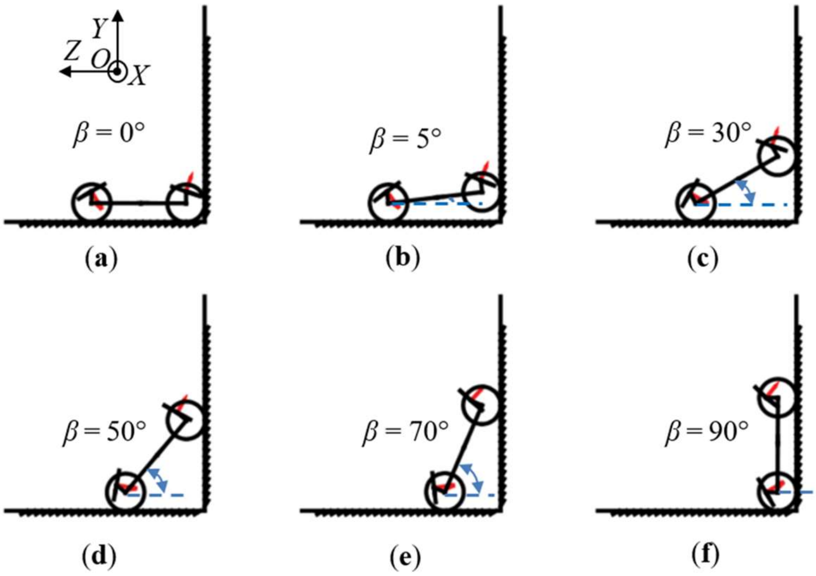

Figure 6. Control strategy of DP-Climb internal transition: (**a**) start transition movement; (**b**) the front wheels raised; (**c**) the angle of the front rotor unit corresponds to the change to ensure an upward force; (**d**) the pitch angle of the body increases, and the adhesion force of the front rotor unit increases; (**e**) the pitch angle of the body exceeds 60 degrees, and the rotor units mainly provide adhesion force; (**f**) complete transition tasks and start wall missions.

When the ranging sensor detects that DP-Climb meets the wall, the robot starts to perform a ground-wall transition motion: the front wheels of the robot start to lift, the front and rear rotor platforms change the pitch angle, and the front rotor unit mainly provides the upward lift force to the robot, the rear rotor unit mainly provides the adhesion force, and the driving wheels mainly provide the power for the robot to move forward on the ground. Then the pitch angle of the fuselage increases and the pitch angle of the front rotor platform decreases correspondingly so that the front rotor platform always provides the upward lift force and the adhesion force pointing to the wall. When the fuselage pitch angle β exceeds 30°, the front rotor platform angle decreases, and the adhesion force provided by the front rotor unit toward the wall increases. When the fuselage pitch angle β exceeds 50°, the front and rear rotor units mainly provide adhesion force pointing to the wall, and the driving wheels mainly provide the power to move forward. Finally, the robot completes the transition task and starts wall operation tasks. Figure 7 shows the pitch angle variation of the robot's front and rear rotor joints in the DP-Climb ground-wall transition control strategy.

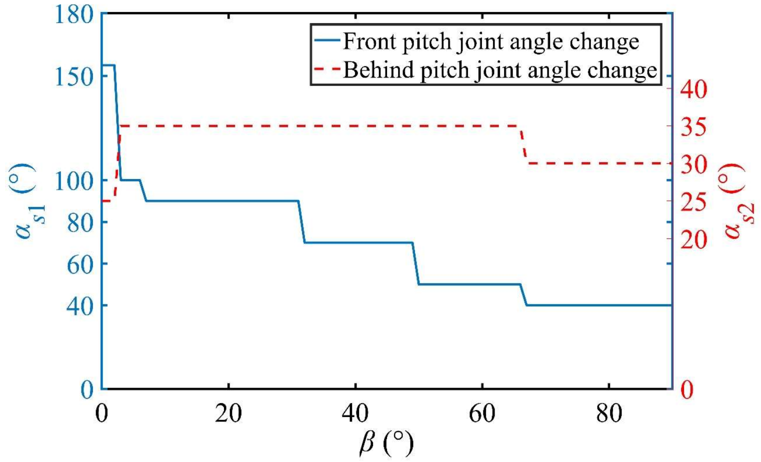

Figure 7. Variation of the pitch angle of the front and behind rotor joints of DP-Climb.

To maintain the stability of the hybrid system and reduce motion error, we introduced the control strategy into the control system. We selected the k_p, k_i and k_d coefficients of the PID controller based on the strategy to adjust the attitude of the robot. v_r and β_r are the desired speed of the robot and the desired pitch angle of the robot, respectively, based on the DP-Climb dynamic model established. The control system of DP-Climb and the PID controller is shown in Figure 8 and Table 2, respectively.

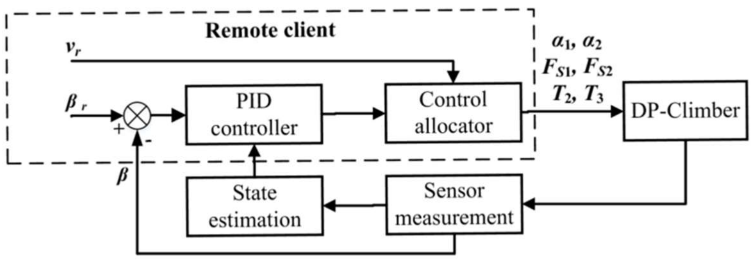

Figure 8. Control system of DP-Climb.

Table 2. k_p, k_i and k_d coefficients selected in the process of ground-wall transition.

Critical Transition Angle β (°)	k_p	k_i	k_d
0	1.80	7.00	1.50
5	1.80	7.60	1.90
30	1.80	7.20	1.90
50	1.80	7.20	1.60
70	1.80	7.00	1.60
90	1.80	7.00	1.50

The inner loop updates the attitude of the robot, the outer loop feedback control reduces the error, the sampling frequency of the inner loop is 10 Hz, and the sampling frequency of the outer loop is 5 Hz.

In summary, in the robot ground-wall transition process, the robot's head-up action mainly relies on the upward lift force provided by the front rotor platform. As the pitch angle of the fuselage increases, α_{s1} gradually decreases, and the adhesion force provided by F_{s1} gradually increases accordingly. The front rotor platform's pitch angle greatly influences the robot's motion, and the changes during the transition motion of the robot are relatively obvious. Thus, the effective output pulling force of the robot rotor unit needs to be analyzed.

3.3.3. Aerodynamic Characteristics of the DP-Climb Adhesion System

DP-Climb performs the transition task, and the wall task mainly relies on the power provided by the adhesion system, according to the analysis above. Based on the established dynamics model of DP-Climb, the output pulling force of the adhesion system required for different pitch angles in transition motion can be obtained. To compensate for the error caused by system interference and airflow disturbance, it is necessary to analyze the actual output of the pulling force of the rotor unit.

First, the robot was fixed by a fixture, and an external current sensor was used to measure the real-time current output of a single rotor unit. A host computer modulated the pulse width of the electronic speed controller of the rotor motor to control the motor speed. Finally, the measured data were collected and analyzed by wireless signal transmission to obtain the pulling force output model of the rotor unit. The aerodynamic characteristics measurement platform of the rotor unit is shown in Figure 9.

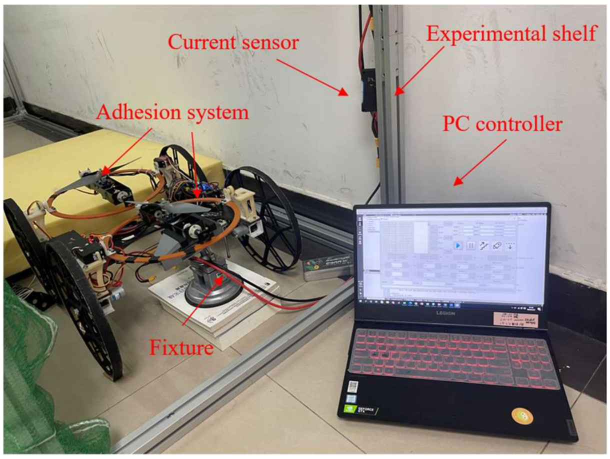

Figure 9. Aerodynamic characteristics measurement platform.

After processing the measured data by linear interpolation, the relationship between the actual current signal of a single rotor unit, the reverse thrust of the rotor and the motor speed can be obtained, as shown in Figure 10.

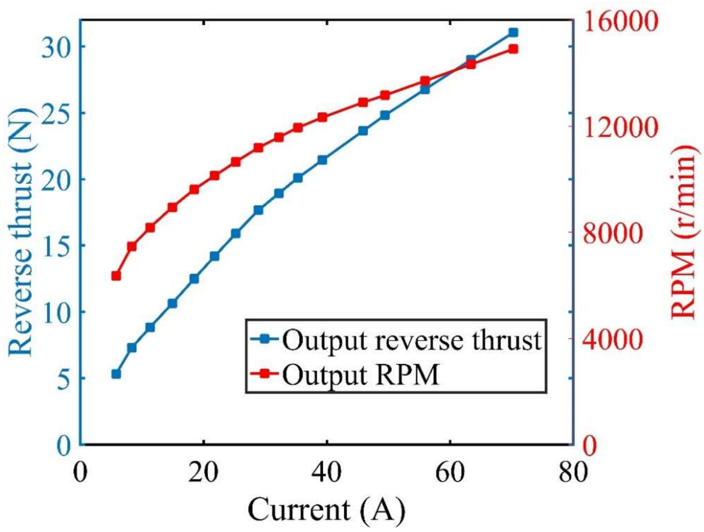

Figure 10. Aerodynamic characteristics of rotor unit.

Since there are two symmetrical rotor units in the robot's adhesion system, there is a certain interference situation when the rotor units act simultaneously, causing decreased pulling force output. Therefore, further analysis of the aerodynamic coupling characteristics of the two rotor units is needed. The RPM of the front and rear rotors were set to 10,653 r/min and 6362 r/min, respectively. Six key nodes of the robot attitude change in the ground-wall transition were selected to simulate the aerodynamic characteristics of the adhesion system at the transition nodes of 0°, 5°, 30°, 50°, 70° and 90° of the fuselage pitch angle. The simulation results of the aerodynamic characteristics of the adhesion system are shown in Figure 11.

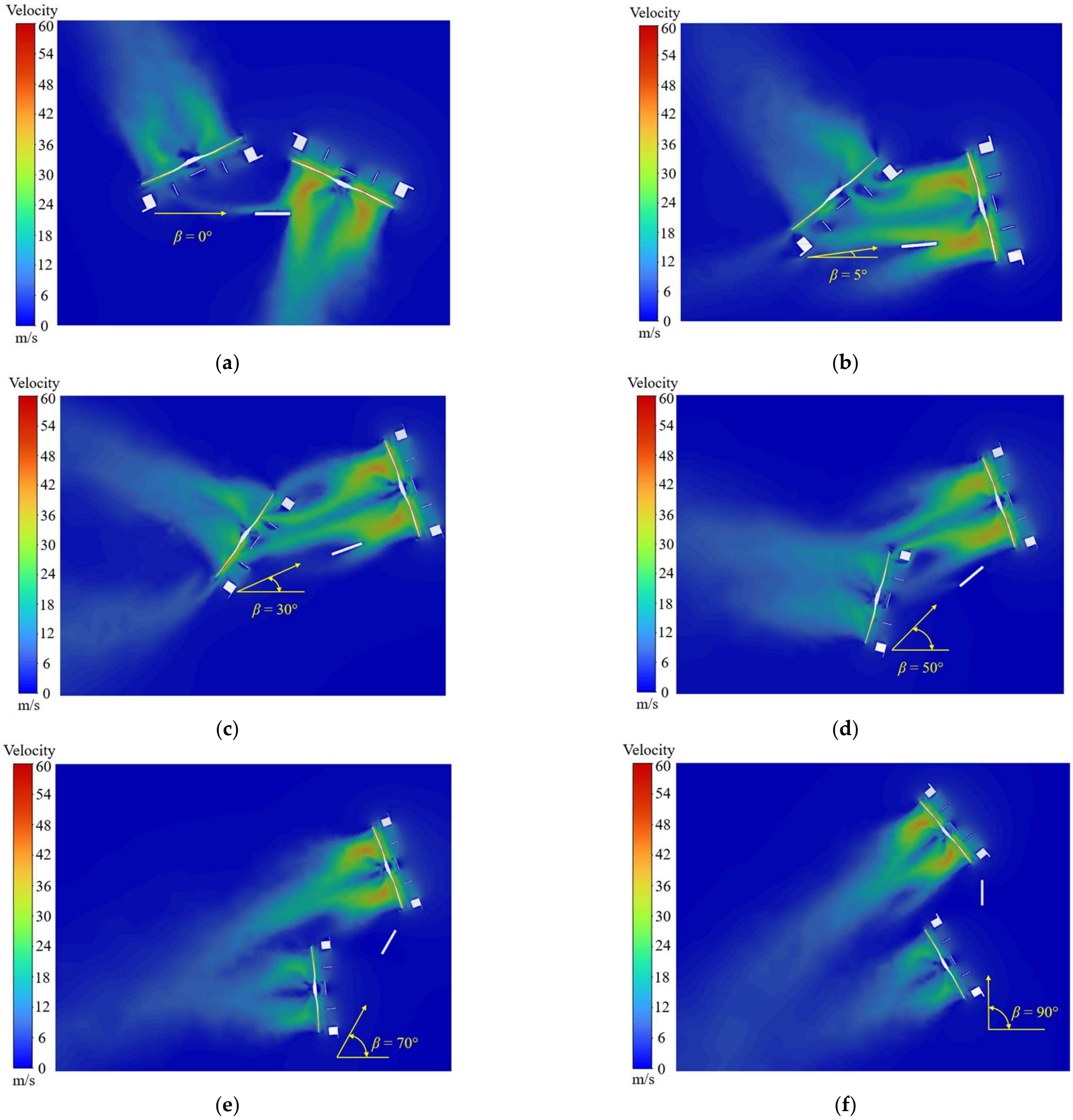

Figure 11. Velocity contours of DP-Climb critical transition nodes: (**a**) β = 0°; (**b**) β = 5°; (**c**) β = 30°; (**d**) β = 50°; (**e**) β = 70°; (**f**) β = 90°.

The relationship between the pitch angle of the robot body and the front and rear rotor platforms is shown in Table 3.

Table 3. Simulation analysis of aerodynamic coupling characteristics of adhesion system.

Rotor Unit	F (N)	Critical Transition Angle β (°)	Rotor Pitch Angle (°)	Simulation Result (N)	Error (%)
Front	15.91	0	155	15.26	4.09
		5	100	15.95	−0.25
		30	90	15.43	3.02
		50	70	15.40	3.21
		70	50	15.50	2.58
		90	40	15.63	1.76
Behind	5.32	0	25	5.53	−3.95
		5	35	5.38	−1.13
		30	35	5.77	−8.46
		50	35	5.53	−3.95
		70	35	5.52	−3.76
		90	30	5.54	−4.14

In summary, the effective pulling force error caused by the mutual coupling effect of the two rotor units is not greater than 8.46%, which can reach the reverse thrust required for the ground-wall transition calculated by the DP-Climb dynamics model. It can be seen that the proposed DP-Climb ground-wall transition strategy is feasible.

4. Discussion

To verify the feasibility of the proposed DP-Climb ground-wall transition control strategy, physical prototype experiments were carried out to validate it and to test the robot's wall operation capability. A nine-axis digital attitude sensor was selected to feed back the robot's attitude change during the ground-wall transition. At the same time, the encoder wheel was used to feed back the robot's displacement in real-time. The movement speeds of different operating postures were measured by combining the returned data information from the sensors.

An experimental safety frame was built to ensure the safety of the robot and the operator, and a safety rope was connected to the robot chassis. The safety rope was completely slack during the movement of the robot and was only used to tighten the rope to prevent accidents under special circumstances. The experiments were divided into three parts to verify the robot motion performance: (1) the transition motion of the ground wall; (2) the variable-speed motion on the wall; and (3) the transition motion of the wall-ground.

(1) Robot ground-wall transition movement. The motion process of the robot is shown in Figure 12. During this motion process, based on the proposed ground-wall transition motion strategy, the motion of the robot was controlled through the hybrid adhesion system of DP-Climb.

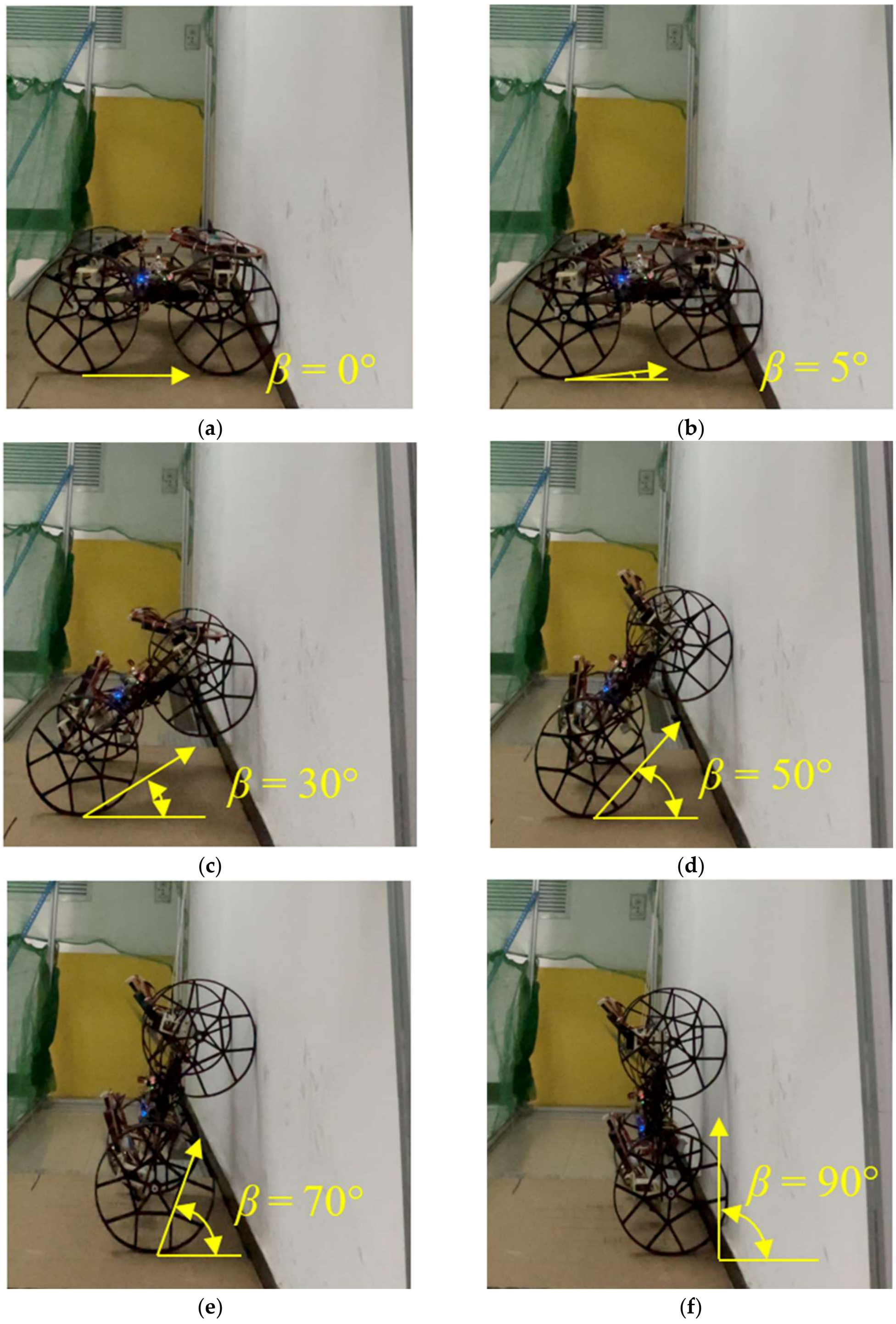

Figure 12. Ground-wall transition experiment of DP-Climb: (**a**) $\beta = 0°$; (**b**) $\beta = 5°$; (**c**) $\beta = 30°$; (**d**) $\beta = 50°$; (**e**) $\beta = 70°$; (**f**) $\beta = 90°$.

Analyzing the data information returned by the sensors, as shown in Figure 12, the robot can adjust the adhesion force and traction force of the rotor units according to its own pitch angle at different stages during the ground-wall transition motion process, which ensures that the robot's adhesion system can provide sufficient power at any angle to meet the motion demand of the robot for a smooth transition between the ground and the wall. The transition speed of the robot during the ground-wall transition is 0.12 m/s.

(2) The variable-speed motion of the robot on the wall. The movement process of the robot is shown in Figure 13. During this movement process, the robot's ability to move flexibly on the wall surface was verified by changing the movement speed and movement state of the robot.

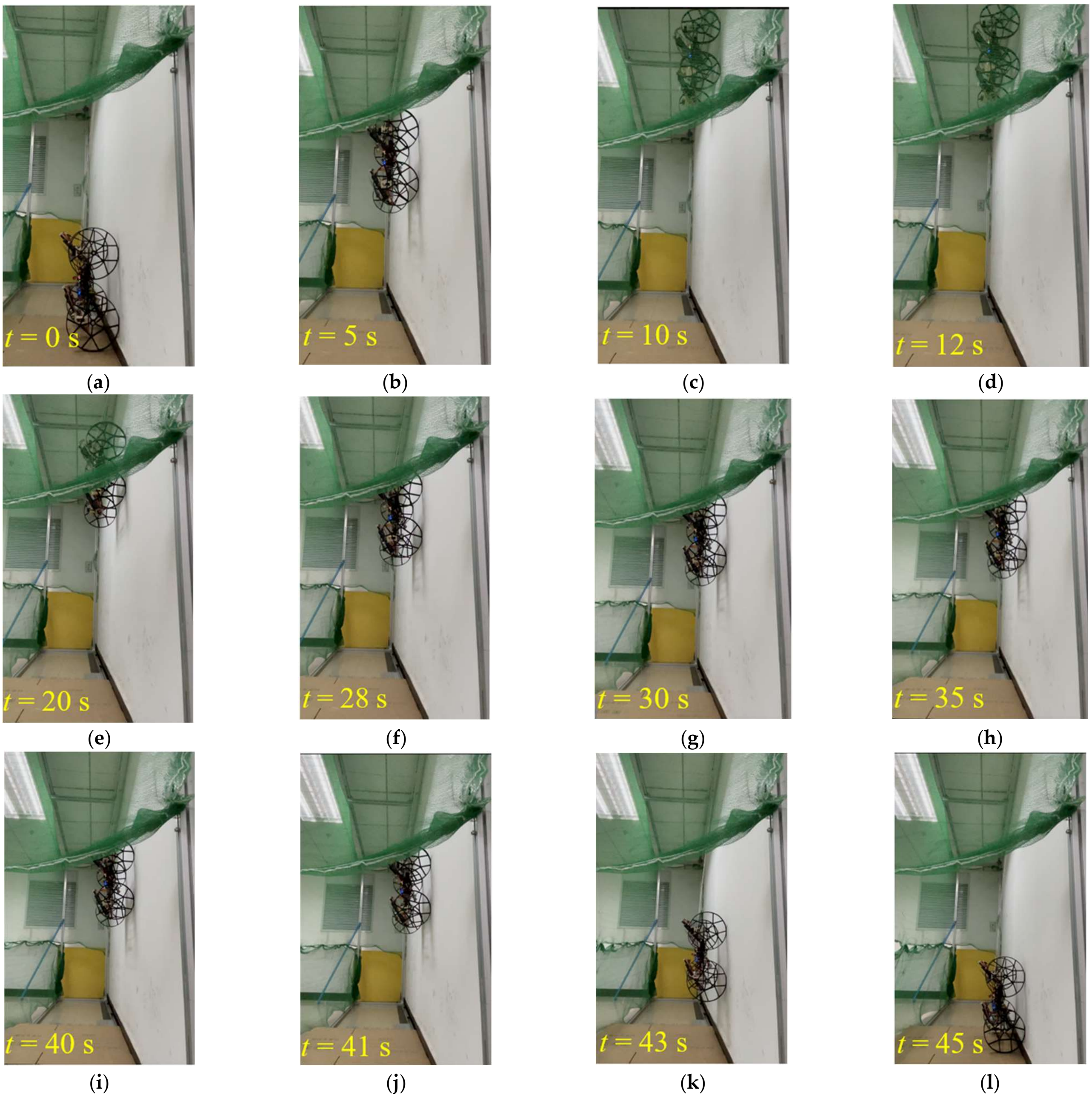

Figure 13. Wall variable-speed forward and backward experiment of DP-Climb: (**a**–**c**) wall forward movement; (**d**–**f**) wall deceleration backward movement; (**g**–**i**) wall static negative pressure adhesion; (**j**–**l**) wall acceleration backward movement.

Analyzing the data information returned by the sensors, as shown in Figure 13, during the robot's variable-speed motion on the wall, the hybrid adhesion system can ensure that the robot meets the safe adhesion conditions on the wall under different motion speeds and accelerations and realize flexible and fast movement on the wall. In Figure 13a–c), the forward speed of the robot was 0.21 m/s. In Figure 13d–f, the robot decelerated and moved backward, and the movement speed was 0.05 m/s. In Figure 13g–i, the robot decelerated to 0 and was kept on the wall with a stable negative pressure. In Figure 13j–l, the robot accelerated and moved backward, and the movement average speed reached 0.25 m/s. The DP-Climb maximum speed can reach 0.45 m/s.

(3) The wall-ground transition of the robot. The movement process of the robot is shown in Figure 14.

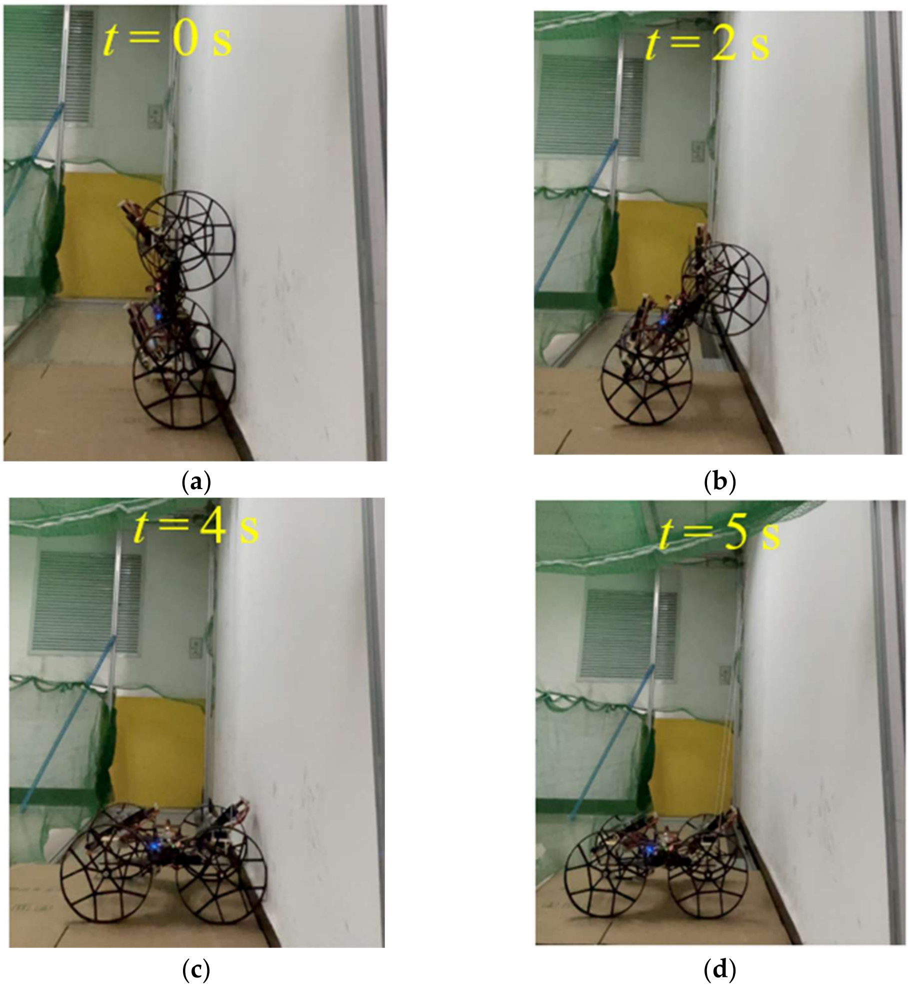

Figure 14. Wall-ground transition experiment of DP-Climb: (**a**) preparation for going down the wall; (**b**) the drive wheels reversed, and the robot went down the wall; (**c**) the robot finished going down the wall; (**d**) the robot walked on the ground.

The experiments can be seen at Supplementary Materials. Analyzing the data information returned by the sensors, as shown in Figure 14a–d, during the wall-ground transition, the robot mainly relies on the rotor units to provide sufficient adhesion force, and the driving wheels mainly provide the traction force of the robot. The transition motion speed of the robot during the wall-ground transition was 0.12 m/s.

5. Conclusions

This paper designed a double propeller wall climbing robot(DP-Climb) with a hybrid adhesion system that can be internally transitioned based on the principle of biomimetic design from the perspective of robot dynamics. The aim was to improve the mobility and adaptability of WCR to complex urban operating environments and expand the application scope of the robot according to the clinging characteristics of different creatures, this paper designed a double propeller wall-climbing robot DP-Climb with a hybrid adhesion system based on the biomimetic design principle. The motion characteristics of the robot in the transition motion inside the ground-wall surface were analyzed, and the robot's safe adhesion conditions in the robot's transition motion process were obtained. Based on the Newton–Euler equations, a DP-Climb ground-wall transition dynamic model was established, and finally, a DP-Climb ground-wall internal transition PID control strategy was introduced. Through mechanical and aerodynamic experiments, it was verified that the effective adhesion force output error of the double propeller symmetric configuration of the robot could converge within 8.46%, and the actual output adhesion force could meet the task requirements of the robot. It can flexibly and rapidly complete the ground-wall transition motion and achieve flexible switching between variable-speed forward, backward, and static adhesion motion states on the vertical wall. The transition motion speed of the robot during the ground-wall transition can reach 0.12 m/s. The wall motion maximum speed can reach 0.45 m/s. The WCR has high maneuverability and flexibility, enabling the robot to quickly complete the specified task in the target area, reducing the time consumed by the robot due to posture adjustment and extending the robot's endurance.

To verify the robot's general adaptability and system stability, the ability of DP-Climb to smoothly transition on the outer surface of the urban building with more severe damage to a slippery wall or the wall will be further studied in the future.

Supplementary Materials: The following supporting information can be downloaded at: https://www.mdpi.com/article/10.3390/machines10080678/s1, Video S1: Ground-wall transition experiment of DP-Climb; Video S2: Wall variable-speed forward and backward experiment of DP-Climb; Video S3: Wall-ground transition experiment of DP-Climb.

Author Contributions: Conceptualization, Q.Z. and X.G.; methodology, Q.Z., X.G. and M.L.; software, Q.Z. and Y.W.; validation, Q.Z., M.L. and Y.W.; formal analysis, Q.Z., M.L. and Y.W.; investigation, Q.Z. and X.G.; resources, Q.Z. and P.L.; data curation, Q.Z. and Y.W.; writing—original draft preparation, Q.Z., X.G. and M.L.; writing—review and editing, Q.Z., X.G; visualization, Q.Z.; supervision, Q.Z. and X.G; project administration, X.G.; funding acquisition, X.G. All authors have read and agreed to the published version of the manuscript.

Funding: This research was funded by the National Key Research and Department Program of China (Grant No. 2019YFB1309600).

Institutional Review Board Statement: Not applicable.

Informed Consent Statement: Not applicable.

Data Availability Statement: Not applicable.

Conflicts of Interest: The authors declare no conflict of interest.

References

1. Ge, D.; Tang, Y.; Ma, S.; Matsuno, T.; Ren, C. A Pressing attachment approach for a wall-climbing robot utilizing passive suction cups. *Robotics* **2020**, *9*, 26. [CrossRef]
2. Chu, B.; Jung, K.; Han, C.-S.; Hong, D. A survey of climbing robots: Locomotion and adhesion. *Int. J. Precis. Eng. Manuf.* **2010**, *11*, 633–647. [CrossRef]
3. Mahmood, S.K.; Bakhy, S.H.; Tawfik, M.A. Novel wall-climbing robot capable of transitioning and perching. *IOP Conf. Ser. Mater. Sci. Eng.* **2020**, *881*, 012049. [CrossRef]
4. Nagaya, K.; Yoshino, T.; Katayama, M.; Murakami, I.; Ando, Y. Wireless piping inspection vehicle using magnetic adsorption force. *IEEE/ASME Trans. Mechatron.* **2012**, *17*, 472–479. [CrossRef]
5. Nansai, S.; Mohan, R. A Survey of wall climbing robots: Recent advances and challenges. *Robotics* **2016**, *5*, 14. [CrossRef]
6. Wang, W.; Wu, S. A caterpillar climbing robot with spine claws and compliant structural modules. *Robotica* **2016**, *34*, 1553–1565. [CrossRef]
7. Chen, R.; Fu, L.; Qiu, Y.; Song, R.; Jin, Y. A gecko-inspired wall-climbing robot based on vibration suction mechanism. *Proc. Inst. Mech. Eng. Part C J. Mech. Eng. Sci.* **2019**, *233*, 7132–7143. [CrossRef]
8. Chattopadhyay, P.; Ghoshal, S.K. Adhesion technologies of bio-inspired climbing robots: A survey. *Int. J. Robot. Autom.* **2018**, *33*, 654–661. [CrossRef]
9. Eto, H.; Asada, H.H. Development of a wheeled wall-climbing robot with a shape-adaptive magnetic adhesion mechanism. In Proceedings of the 2020 IEEE International Conference on Robotics and Automation (ICRA), Online Conference, 31 May–31 August 2020; pp. 9329–9335.

10. Zhu, H.; Guan, Y.; Wu, W.; Zhang, L.; Zhou, X.; Zhang, H. Autonomous pose detection and alignment of suction modules of a biped wall-climbing robot. *IEEE/ASME Trans. Mechatron.* **2015**, *20*, 653–662. [CrossRef]
11. Liu, Y.; Kim, H.; Seo, T. AnyClimb: A new wall-climbing robotic platform for various curvatures. *IEEE/ASME Trans. Mechatron.* **2016**, *21*, 1812–1821. [CrossRef]
12. Liu, Y.; Seo, T. AnyClimb-II: Dry-adhesive linkage-type climbing robot for uneven vertical surfaces. *Mech. Mach. Theory* **2018**, *124*, 197–210. [CrossRef]
13. Bian, S.; Xu, F.; Wei, Y.; Kong, D. A Novel type of wall-climbing robot with a gear transmission system arm and adhere mechanism inspired by cicada and gecko. *Appl. Sci.* **2021**, *11*, 4137. [CrossRef]
14. Liang, P.; Gao, X.; Zhang, Q.; Li, M.; Gao, R.; Xu, Y. Analysis and experimental research on motion stability of wall-climbing robot with double propellers. *Adv. Mech. Eng.* **2021**, *13*, 16878140211047726. [CrossRef]
15. Cho, K.J.; Koh, J.S.; Kim, S.; Chu, W.S.; Hong, Y.; Ahn, S.H. Climbing robots for commercial applications—A survey. *Int. J. Precis. Eng. Manuf.* **2009**, *10*, 171–181. [CrossRef]
16. Kim, H.; Kim, D.; Yang, H.; Lee, K.; Seo, K.; Chang, D.; Kim, J. Development of a wall-climbing robot using a tracked wheel mechanism. *J. Mech. Sci. Technol.* **2009**, *22*, 1490–1498. [CrossRef]
17. Fu, Y.; Li, Z.; Wang, S. A Wheel-leg hybrid wall climbing robot with multi-surface locomotion ability. In Proceedings of the 2008 IEEE International Conference on Mechatronics and Automation, Takamatsu, Japan, 5–8 August 2008; pp. 627–632.
18. Koo, I.M.; Trong, T.D.; Lee, Y.H.; Moon, H.; Koo, J.; Park, S.K.; Choi, H.R. Development of wall climbing robot system by using impeller type adhesion mechanism. *J. Intell. Robot. Syst.* **2013**, *72*, 57–72. [CrossRef]
19. Wang, Y.; Liu, S.; Xu, D.; Zhao, Y.; Shao, H.; Gao, X. Development and application of wall-climbing robots. In Proceedings of the 2013 IEEE/RSJ International Conference on Intelligent Robots and Systems, Tokyo, Japan, 3–7 November 2013; pp. 1207–1212.
20. Schmidt, D.; Berns, K. Climbing robots for maintenance and inspections of vertical structures—A survey of design aspects and technologies. *Robot. Auton. Syst.* **2013**, *61*, 1288–1305. [CrossRef]
21. Myeong, W.; Song, S.; Myung, H. Development of a wall-climbing drone with a rotary arm for climbing various-shaped surfaces. In Proceedings of the 2018 15th International Conference on Ubiquitous Robots, Honolulu, HI, USA, 26–30 June 2018; pp. 687–692.
22. Ma, B.; Liu, R.; Zhang, R.; Tian, L. Design of wall climbing robots with transition capability. In Proceedings of the 2007 IEEE International Conference on Robotics and Biomimetics (ROBIO), Sanya, China, 15–18 December 2007; pp. 1871–1875.
23. Dong, W.; Wang, H.; Li, Z.; Jiang, Y.; Xiao, J. Development of a wall-climbing robot with biped-wheel hybrid locomotion mechanism. In Proceedings of the 2013 IEEE/RSJ International Conference on Intelligent Robots and Systems, Tokyo, Japan, 3–7 November 2013; pp. 2333–2338.
24. Zhao, X.; Zhang, Q.; Wang, L.; Xie, F.; Zhang, B. A Special operation UAV in urban space. In Proceedings of the Applied Optics and Photonics China 2021, Beijing, China, 23–25 July 2021; Volume 12065, pp. 433–442.
25. Ioi, K.; Yokoi, H.; Kimura, M. Development of a compact and rapid wall-climber. In Proceedings of the 2013 18th International Conference on Methods & Models in Automation & Robotics (MMAR), Międzyzdroje, Poland, 26–29 August 2013; pp. 344–349.
26. Lee, G.; Kim, H.; Seo, K.; Kim, J.; Kim, H.S. MultiTrack: A multi-linked track robot with suction adhesion for climbing and transition. *Robot. Auton. Syst.* **2015**, *72*, 207–216. [CrossRef]
27. Liang, P.; Gao, X.; Gao, R.; Zhang, Q.; Li, M. Analysis of the aerodynamic performance of a twin-propelled wall-climbing robot based on computational fluid dynamics method. *AIP Adv.* **2022**, *12*, 015022. [CrossRef]
28. Liang, P.; Gao, X.; Zhang, Q.; Gao, R.; Li, M.; Xu, Y.; Zhu, W. Design and stability analysis of a wall-climbing robot using propulsive force of propeller. *Symmetry* **2020**, *13*, 37. [CrossRef]
29. Alkalla, M.G.; Fanni, M.A.; Mohamed, A.M.; Hashimoto, S. Tele-operated propeller-type climbing robot for inspection of petrochemical vessels. *Ind. Robot Int. J.* **2017**, *44*, 166–177. [CrossRef]
30. Alkalla, M.G.; Fanni, M.A.; Mohamed, A.F.; Hashimoto, S.; Sawada, H.; Miwa, T.; Hamed, A. EJBot-II: An optimized skid-steering propeller-type climbing robot with transition mechanism. *Adv. Robot.* **2019**, *33*, 1042–1059. [CrossRef]
31. Myeong, W.; Myung, H. Development of a wall-climbing drone capable of vertical soft landing using a tilt-rotor mechanism. *IEEE Access* **2019**, *7*, 4868–4879. [CrossRef]
32. Han, I. Development of a stair-climbing robot using springs and planetary wheels. *Proc. Inst. Mech. Eng. Part C J. Mech. Eng. Sci.* **2008**, *222*, 1289–1296. [CrossRef]
33. Oliveira, A.L.C.; Silva, M.F.; Barbosa, R.S. Architecture of an wheeled climbing robot with dynamic adjustment of the adhesion system. In Proceedings of the SISY 2010: IEEE 8th International Symposium on Intelligent Systems and Informatics, Subotica, Serbia, 10–11 September 2010; pp. 127–132.
34. Zhang, L.; Sun, J.; Yin, G.; Zhao, J.; Han, Q. A Cross Structured Light Sensor and Stripe Segmentation Method for Visual Tracking of a Wall Climbing Robot. *Sensors* **2015**, *15*, 13725–13751. [CrossRef]
35. Ding, X.; Yu, Y.; Zhu, J.J. Trajectory linearization tracking control for dynamics of a multi-propeller and multifunction aerial robot-MMAR. In Proceedings of the 2011 IEEE International Conference on Robotics and Automation (ICRA), Shanghai, China, 9–13 May 2011; pp. 757–762.
36. Nishi, A.; Miyagi, H. Mechanism and control of propeller type wall-climbing robot. In Proceedings of the IEEE/RSJ International Conference on Intelligent Robots and Systems (IROS'94), Munich, Germany, 12–16 September 1994; Volume 3, pp. 1724–1729.

37. Hawkes, E.W.; Eason, E.V.; Christensen, D.L.; Cutkosky, M.R. Human climbing with efficiently scaled gecko-inspired dry adhesives. *J. R. Soc. Interface* **2015**, *12*, 20140675. [CrossRef]
38. Yu, J.; Chary, S.; Das, S.; Tamelier, J.; Pesika, N.S.; Turner, K.L.; Israelachvili, J.N. Gecko-inspired dry adhesive for robotic applications. *Adv. Funct. Mater.* **2011**, *21*, 3010–3018. [CrossRef]